PRESSURE-DRIVEN PHASE CHANGE MODEL FOR INTERFACIAL MASS TRANSFER IN AIR-WATER SYSTEMS

by

Rong XIAO[a], Peifa MA[a], Tong ZHU[a*], Feng SU[b], Lu WANG[c], and Ying CHI[c]

[a]School of Mechanical Engineering, Tongji University, Shanghai, China
[b]Southwest Municipal Engineering Design and Research Institute of China, Chengdu, Sichuan, China
[c]China Nuclear Power Engineering Co., Ltd., Beijing, China

Original scientific paper
https://doi.org/10.2298/TSCI251003240X

The Lee model uses saturation temperature as the only criterion for phase change and does not consider the dynamic influence of vapour partial pressure. This paper addresses the dry air-water system at 0-60 °C by incorporating a vapour pressure gradient source term via a user-defined function within the VoF interface capture framework. This construct enhances the gas-liquid mass transfer model by dynamically updating the saturated vapour pressure via temperature-dependent expressions. The simultaneous coupling of temperature and humidity gradients enables a more comprehensive characterization of the thermodynamics of low temperature evaporation, thus broadening the applicability of the model and enabling it to better approximate real-world physical processes. Systematic investigation of the mass transfer characteristics of the phase change mass transfer coefficient, β, over five orders of magnitude (from 10^{-1}-10^{-5}) revealed the behavior of the key control mechanisms. In the high phase change mass transfer coefficient region ($\beta > 10^{-3}$), the evaporation mass transfer rate is primarily controlled by the vapour pressure difference, whereas in the low phase change mass transfer coefficient region ($\beta < 10^{-3}$), the evaporation mass transfer process is dominated by β. Using parameter inversion with independent experimental data, the optimal range for the phase change mass transfer coefficient, β, in low temperature evaporation simulations of dry air-water single-pore bubble systems was determined to be 10^{-4}-10^{-5}. The developed model provides an optimized framework for simulating phase change mass transfer in low temperature evaporation processes.

Keywords: *VoF model, gas-liquid interface, evaporation model, mass transfer coefficient*

Introduction

Gas-liquid mass transfer is an important research topic in engineering and science. Its mass transfer mechanism exhibits significant composition dependence, and when phase change mass transfer occurs between the gas and liquid phases, the vapour concentration at the interface is in a non-equilibrium state, resulting in discontinuous to ensure the continuity of

*Corresponding author, e-mail: zhu_tong@tongji.edu.cn

pressure and temperature [1]. In air-water systems, the difference between the partial pressure of water vapour and the saturation vapour pressure at the liquid surface is the key driving force for mass transfer. Experimental evidence indicates that in the temperature range of 20-50 °C, the saturation vapour pressure of water increases exponentially from 2.34 kPa to 12.34 kPa, a 5.3-fold increase [2]. The temperature dependence of saturation vapour pressure is of particular significance under non-isothermal conditions. Minor temperature variations have been shown to induce substantial changes in saturation vapour pressure, thereby critically influencing mass transfer processes. Therefore, in the study of mass transfer between gases and liquids under nonuniform temperature conditions, it is necessary to account for the thermal vapour pressure coupling.

Numerical simulations have become indispensable for studying gas-liquid heat and mass transfer owing to their computational efficiency and flexibility. For gas-liquid multiphase systems. Among these, the mixed model assumes local velocity-temperature equilibrium within each phase, requiring only a single set of conservation equations supplemented by algebraic slip corrections. It exhibits minimal computational demands and is suitable for dilute systems characterized by low discrete phase volume fractions, small particle sizes, and weak interphase slip. However, its neglect of interfacial area density precludes the analysis of interfacial thermodynamic states required for evaporation and condensation, rendering it appropriate solely for rapid estimation. In contrast, the two-fluid model establishes separate momentum and continuity equations for each phase, coupled through source terms such as drag, lift, and virtual mass. This approach captures phenomena like large slip, agglomeration, and countercurrent flow, thus making it applicable to high-load, strong interphase interaction scenarios such as bubble columns and fluidized beds. However, this doubles the number of equations and requires closure of interphase exchange terms; it is sensitive to the mesh, time step, and closure model, demanding the highest computational resources, yet remains unparalleled in accuracy and information content. The VoF model employs a single set of momentum equations and volume fraction transport equations. It captures sharp phase interfaces through piecewise linear geometric reconstruction, rigorously ensuring global mass conservation, and is suitable for conditions requiring explicit analysis of interface topology, such as free surfaces, stratified flows, and large-scale bubbles or droplets.

The VoF method is widely used for simulating multiphase flows [3], demonstrating strong performance in capturing bubble dynamics [4, 5]. The method has been extensively validated in heat and mass transfer studies for accurately tracking gas-liquid interface evolution [6-8]. For phase change mass transfer, the computationally efficient Lee model is commonly used due to its simplicity and suitability for near-saturation conditions where phase change dominates [9, 10]. To enhance practical applications, the VoF method is often coupled with the Lee model [11-13].

However, the Lee model's constant saturation temperature assumption restricts its capability to capture dynamic mass transfer at phase interfaces. Some research groups have developed modifications to overcome this constraint. Zhang *et al*. [14] proposed an improved phase change model based the Lee model, enhancing computational efficiency and numerical stability via interfacial energy redistribution. Their mass and energy source term model shows substantial improvement compared to the original Lee model. Shen *et al*. [15] investigated interfacial heat transfer with the Lee model, proposing a vapour thermal conductivity correction for the two-phase region. They developed a modified condensation model and validated it against Nusselt theoretical solutions for liquid film thickness. It is imperative to emphasize that the phase change mass transfer coefficient, β, as the pivotal empirical parameter in the Lee

model, can be determined empirically without the necessity of complex theoretical derivation. In this model, higher β values generally provide enhanced congruence with physical reality, however, values that are excessively large may result in convergence challenges. The typical range for β is 10^{-1}-10^{7} s^{-1} [9, 16] , with recommended values down to 0.1 s^{-1} for evaporation processes and up to 10^{6} s^{-1} for condensation simulations.

Alizadehdakhel *et al*. [17] established a two-phase flow model for thermal siphon tubes, with a phase change mass transfer coefficient of 0.1 s^{-1}. The numerical results obtained from this model demonstrated excellent agreement with experimental measurements. Cheng *et al*. [18] integrated numerical simulation (phase change mass transfer coefficient β = 0.5 s^{-1}) with experimental investigations to elucidate flow and heat transfer characteristics governed by saturated-nucleate boiling in vertical confined rectangular channels under low-heat-flux conditions. This study established theoretical foundations for narrow-channel heat exchanger design. Luo *et al*. [19] employed evaporative and condensation mass transfer coefficients of 10^{2} s^{-1} and 10^{6} s^{-1}, respectively, in order to address challenges in the convergence of flow boiling simulations within manifold micro-channels. In air-water evaporation systems, the driving force for mass transfer is the vapour pressure difference between unsaturated air and the saturated vapour layer at the liquid interface. However, the temperature difference has been found to be inadequate for accurately capturing the actual mass transfer dynamics at the interface. Chen *et al*. [20] developed a modified formulation of the Lee model by replacing the normalized temperature difference with a temperature difference in the source term calculations, thereby eliminating the uncertainties arising from the denominator. By integrating this improved phase change mass transfer model with the VoF method, they were able to implement it effectively for condensation simulations in rectangular microchannels, yielding improved numerical solutions for microscale phase change mass transfer problems.

The VoF model employs a volume fraction transport equation to capture phase boundaries, enabling precise analysis of sharp interfaces, deformation, and area dynamics while rigorously ensuring both global and local mass conservation. This makes it indispensable for phase-change mass transfer processes such as evaporation. Given the stringent demands of evaporation mass transfer on interface accuracy and mass conservation, the VoF model was selected for this numerical simulation.

The Lee model is predicated on the fundamental principle of phase change, with the occurrence of phase change mass transfer being determined by the comparison of fluid temperature with saturation temperature. This model is inadequate in its inability to capture the underlying physical mechanisms. In the context of air-water system evaporation processes, the driving force for mass transfer is derived from the differential between the water vapour partial pressure and the saturation vapour pressure at the liquid surface temperature (*i.e*., the vapour pressure difference). It is evident that the temperature difference is an inadequate characterization of the interfacial mass transfer dynamics. Wang *et al*. [21] developed a pressure-based phase change model and validated the phase change mass transfer coefficient through thermosyphon experiments using ammonia. Liu *et al*. [22] proposed an enhanced Lee model based on the distinct evaporation-condensation characteristics of gravity heat pipes, with a specific analysis of the phase-change mass transfer coefficient to elucidate gas-liquid interfacial mass transfer phenomena in such systems.

In light of this, the present study retains the Lee model's advantages of structural simplicity, single-parameter adjustability, and strict mass-energy conservation. By employing a user-defined function (UDF), the mass transfer driving force is modified to reflect vapour pressure difference, whilst simultaneously incorporating the synergistic effects of temperature

and humidity differentials on phase-change mass transfer to enhance simulation accuracy. For low-temperature evaporation conditions [23], a phase-change model driven by vapour pressure difference is constructed to improve the predictive accuracy of gas-liquid mass transfer processes in dry air-water systems. This model utilizes vapour pressure difference as the mass transfer driving force. The selection of an appropriate empirical correlation is based on the operating temperature range for the purpose of performing dynamic calculations of saturation vapour pressure. Furthermore, in consideration of the physical characteristics of the evaporation process, the computational domain is confined to the gas-liquid interface with a view to enhancing computational efficiency and convergence. A sensitivity analysis of the phase change mass transfer coefficient is conducted based on this model. This analysis provides a preliminary determination of the order of magnitude of the phase change mass transfer coefficient, β, in single-pore bubble low temperature evaporation numerical simulations. This provides a reference basis for numerical simulation studies of simultaneous heat and mass transfer between gas and liquid phases.

In summary, this study focuses on coupled heat and mass transfer during direct gas-liquid contact processes. It constructs and refines an evaporation-condensation phase change model, aiming to provide more precise modelling tools for research into two-phase heat and mass transfer. These tools support performance enhancement and structural optimization in direct evaporative cooling air conditioning systems, intensified mass transfer in aerodynamic agitation systems, and flow pattern regulation in gas-liquid mass transfer equipment. Through simulation techniques, it addresses the limitations of experimental methods in obtaining critical information such as internal flow fields and interfacial concentrations, while reducing research and development costs and cycles.

Phase change model

Lee model

Currently, the widely used Lee model for calculating per-unit-volume boiling or condensation mass transfer rates is primarily based on the temperature gradient, expressed as [24]:

$$S = -\beta\alpha_l\rho_l\frac{T - T_{sat}}{T_{sat}}, \quad T \geq T_{sat}, \; S = \beta\alpha_v\rho_v\frac{T_{sat} - T}{T_{sat}}, \quad T < T_{sat} \tag{1}$$

where S [kgm^{-3}s^{-1}] is the mass source term in the liquid phase continuity equation, β [s^{-1}] – the phase change mass transfer coefficient, α_l and α_v – the volume fractions of the liquid and gas phases, respectively, ρ_l and ρ_v [kgm^{-3}] – the densities of the liquid and gas phases, respectively, T [K] – the fluid temperature, and T_{sat} [K] – the saturation temperature at the vapour partial pressure.

The model defines the phase change interaction term according to the normalized temperature difference; the difference between the local fluid temperature and the saturation temperature ($\Delta T = T_{sat} - T$) is used to determine whether a phase change will occur. In the event of the local fluid temperature, T, being higher than the currently set saturation temperature T_{sat} ($\Delta T < 0$), the conditions for evaporation are met, conversely, when the local fluid temperature, T, is lower than the saturation temperature T_{sat} ($\Delta T > 0$), the conditions for condensation are met. The value of β has a significant impact on the rate and extent of the phase change process. However, the Lee model simplifies the process by using a constant saturation temperature, T_{sat}, and disregards the significant influence of water vapour partial pressure on phase change mass transfer processes, which limits its applicability in evaporation mass transfer simulations.

Evaporation is defined as a mild vaporization phenomenon that occurs exclusively at the gas-liquid interface and is primarily controlled by surface temperature and vapour pressure gradients. In contrast, boiling is defined as an intensive vaporization process that requires reaching the saturation temperature and occurs simultaneously within the liquid and at its surface. The phenomenon is distinguished by its intricate phase change behavior, which encompasses the processes of bubble nucleation and growth. This fundamental difference poses challenges for the traditional Lee model in accurately capturing the unique physical mechanisms of the evaporation process.

Vapour pressure difference driven low temperature evaporation model

The present study proposes an enhanced low temperature phase-change model for the interfacial evaporation mass transfer characteristics in a sub-saturated condition, as shown in fig. 1. The model is based on Lee's mass and energy transfer theory, and its core feature is to restrict phase change mass transfer to occur exclusively within the gas-liquid interface region. The direction of mass transfer is determined by the pressure difference between saturation vapour pressure and water vapour partial pressure ($\Delta P = P_{sat} - P_v$), coupled with temperature-dependent dynamic behavior of saturation vapour pressure. This fundamentally distinguishes it from traditional boiling models. This model specifically considers the interface evaporation mechanism, utilizing the Lee model source term solution framework and coupling it with the dual volume fraction criterion from the VoF method (liquid phase volume fraction $\alpha_l < 0.99$ and gas phase volume fraction $\alpha_v > 0.0001$) to precisely identify the phase interface. This modelling approach not only more accurately describes the interfacial characteristics of the evaporation process but also effectively improves the numerical convergence.

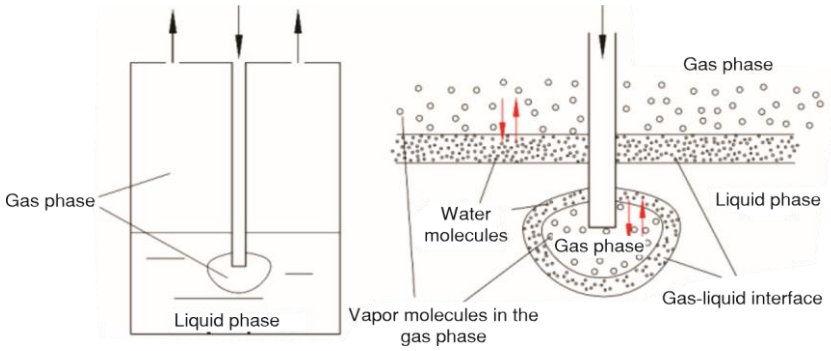

Figure 1. Simple schematic diagram of evaporation process at gas-liquid interface

For mass transfer processes involving direct air-water contact under non-equilibrium conditions, an improved low temperature evaporation model has been established. This model uses the dynamic equilibrium relationship between the local water vapour partial pressure and the saturation vapour pressure at the corresponding temperature as the mass transfer criterion for evaporation and condensation, as shown in tab. 1. In numerical simulations, a computational framework with the liquid phase as the primary phase and the gas phase as the secondary phase was adopted. Based on the latent heat of vaporization corresponding to the initial temperatures of the gas-liquid two-phase system (20 °C) and the inlet gas temperature (50 °C), the average value was taken as 2418 kJ/kg [25].

Table 1. Source term transfer equations based on water vapour pressure difference

Type of transfer	Phase change	Phase	Source term
Mass transfer	Evaporation: $P_v < P_{sat}$	Gas phase	$S = \beta_e \alpha_l \rho_l \left\| \frac{P_{sat} - P_v}{P_{sat}} \right\|$
		Liquid phase	$S = -\beta_e \alpha_l \rho_l \left\| \frac{P_{sat} - P_v}{P_{sat}} \right\|$
	Condensation: $P_v > P_{sat}$	Gas phase	$S = -\beta_e \alpha_v \rho_v \left\| \frac{P_{sat} - P_v}{P_{sat}} \right\|$
		Liquid phase	$S = \beta_e \alpha_v \rho_v \left\| \frac{P_{sat} - P_v}{P_{sat}} \right\|$
Energy transfer	Evaporation: $P_v < P_{sat}$	–	$S = -\beta_e \alpha_l \rho_l \left\| \frac{P_{sat} - P_v}{P_{sat}} \right\| \Delta H$
	Condensation: $P_v > P_{sat}$	–	$S = \beta_e \alpha_v \rho_v \left\| \frac{P_{sat} - P_v}{P_{sat}} \right\| \Delta H$

It is worth noting that to address the issue of FLUENT software being unable to directly obtain the partial pressure of water vapour, this study derived the molar fraction of water vapour through the conversion relationship between the mass fraction and molar mass of water vapour, thereby obtaining the required partial pressure parameters of water vapour. Additionally, considering the constraining effect of saturation vapour pressure on mass transfer processes, since saturation vapour pressure is a function of temperature and exhibits significant variations within the study range, accurately calculating saturation vapour pressure is crucial for quantitatively characterizing mass transfer driving forces. Therefore, this study employs the following saturation vapour pressure calculation formula for the low-temperature range (0-60 °C) [26]:

$$P_{sat} = 133.32 \exp\left(\frac{8.10765 - 1750.286}{T + 235.0}\right) \tag{2}$$

where P_{sat} [Pa] is the saturation vapour pressure and T [K] – the fluid temperature.

Geometric model and boundary conditions

Geometric modelling and mesh generation

The geometric model is a rectangular cavity with dimensions of 300 mm (length) × 150 mm (width) × 400 mm (height). The inlet pipe has a length of 350 mm, with an inlet hole diameter of 20 mm and an outlet hole diameter of 20 mm. The FLUENT MESHING was used to perform mesh partitioning on the geometric model. The geometric model and mesh partitioning are shown in fig. 2.

Based on the low temperature evaporation model proposed in this paper, the numerical reliability was verified through grid independence validation. Sensitivity analysis of the phase change mass transfer coefficient, β, indicated that a reasonable range for numerical simulation

of single air-bubble mass transfer processes is 10^{-4}-10^{-5}, see sections *Phase change model*, hence $\beta = 10^{-4}$ was selected as the validation benchmark parameter. As shown in fig. 3 when the number of grid cells increased from 25383-41287, the deviation in the exit air mass fraction was 0.022, indicating that the initial grid resolution was insufficient. When the mesh count was further increased to 86915, the deviation decreased to 0.002, indicating that the 41287 cell mesh satisfied the grid independence criterion. Therefore, this mesh scheme was ultimately adopted.

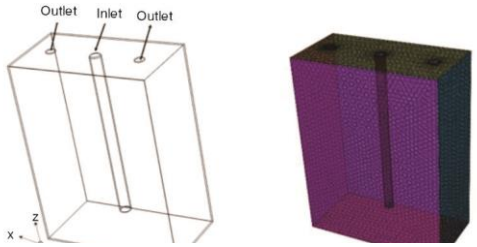

Figure 2. Geometric model (a) and fluid domain mesh partitioning (b)

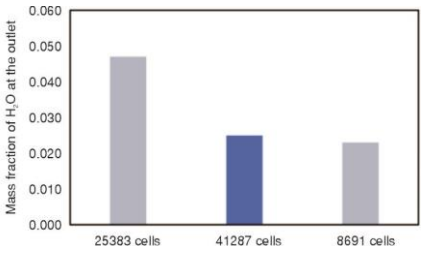

Figure 3. Grid independence verification

Simulation set-up and boundary conditions

Numerical simulation of the heat and mass transfer process in an air-water two-phase system within a rectangular bubble column was conducted using FLUENT 2024 R1. The numerical calculations employed a pressure-based transient solver combined with the SIMPLE algorithm, with a time step of 0.0001 seconds. To describe the dynamic evolution of the gas-liquid interface, the VoF model was selected, which can clearly capture the gas-liquid phase interface. The standard k-ε turbulence model was adopted, as was the surface tension model [27], with the surface tension coefficient set to 0.072 N/m. The species transport model was enabled to track the water vapour diffusion process. The boundary conditions are set as: air inlet velocity is 3 m/s, initial water level is 150 mm, water temperature is 293.15 K, and all walls are set as adiabatic walls. Specifically, this study implements the numerical calculation of the evaporation process through a UDF to more accurately describe the evaporation mass transfer behavior.

The rationale for selecting the standard k-ε model lies in: turbulent kinetic energy, k, and dissipation rate, ε, respectively, characterize pulsation velocity and characteristic length, with the two-equation transport automatically reflecting flow history. The vorticity coefficient $\nu_t = C_\mu k^2/\varepsilon$ combined with the Boussinesq assumption, enables closure of the Reynolds stresses without requiring empirical lengths, offering a concise formulation and numerical robustness. This model provides statistically sufficient turbulent viscosity with only two transport equations under engineering grids, balancing computational efficiency and accuracy. Consequently, it serves as a reliable turbulence closure scheme for simulating evaporation-condensation in gas-liquid two-phase flows dominated by interface dynamics.

Analysis of phase change mass transfer coefficient

In single-hole bubbling experiments in a dry air-water system, the volumetric mass transfer coefficient ranges approximately from 0.01-0.5 s^{-1}. Based on this range, using the formula in the literature [28], the mass fraction range of water vapour in the outlet wet air can be reasonably estimated, thereby providing a strong reference basis for determining the phase

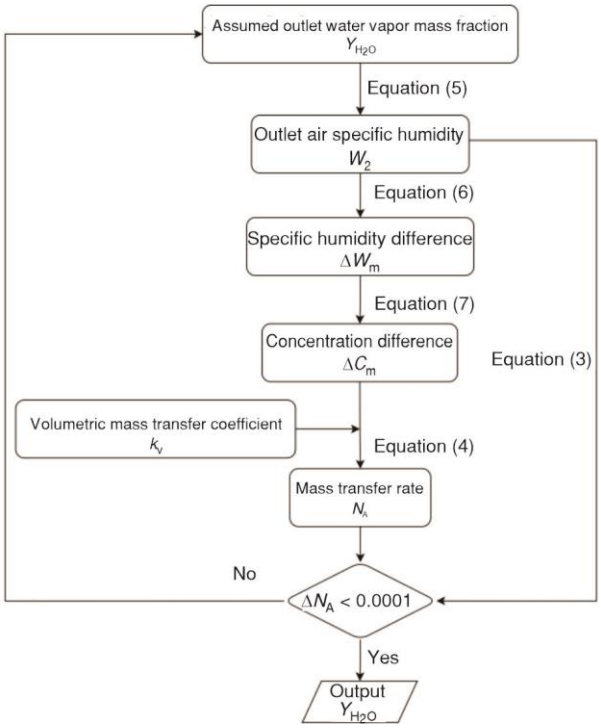

Figure 4. Flowchart for calculating water vapour content at the outlet

Table 2. Mass fraction of outlet water vapour for different volumetric mass transfer coefficients

Symbol [unit]	Numerical value					
Y_{H2O} [–]	0.0262	0.0250	0.0200	0.0150	0.0100	0.0030
W_2 [kgkg^{-1}]	0.0269	0.0256	0.0204	0.0152	0.0101	0.0030
W_1 [kgkg^{-1}]	0	0	0	0	0	0
W_s [kgkg^{-1}]	0.027	0.027	0.027	0.027	0.027	0.027
ΔW_m [kgkg^{-1}]	–0.0051	–0.0086	–0.0145	–0.0183	–0.0216	–0.0255
ρ_g [kg·m^{-3}]	1.16	1.16	1.16	1.16	1.16	1.16
M_{H2O} [kg·mol]	0.018	0.018	0.018	0.018	0.018	0.018
ΔC_m [molm^{-3}]	–0.3285	–0.5541	–0.9349	–1.1849	–1.3924	–1.6450
$\dot{m}_G$ [kgs^{-1}]	0.0011	0.0011	0.0011	0.0011	0.0011	0.0011
N_A [mols^{-1}]	–0.0016	–0.0016	–0.0012	–0.0009	–0.0006	–0.0002
V_1 [m^3]	0.01	0.01	0.01	0.01	0.01	0.01
k_V [s^{-1}]	0.50	0.28	0.13	0.08	0.04	0.01

change mass transfer coefficient, β, in the low temperature phase change mass transfer model. The calculation process is shown in fig. 4, and the specific calculation results are presented in tab. 2:

$$N_A = \frac{\dot{m}_G (W_1 - W_2)}{M_{H_2O}} \tag{3}$$

$$N_A = k_V V_l \Delta C_m \tag{4}$$

$$W_2 = \frac{Y_{H_2O}}{1 - Y_{H_2O}} \tag{5}$$

where N_A [mols^{-1}] is the mass transfer rate and $\dot{m}_G$ [kgs^{-1}] – the mass-flow rate of the inlet air.

The mixing ratio of water vapor is defined as the mass of water vapor contained in a unit mass of dry air, denoted by W, W_1, and W_2 [kgkg^{-1}] denote the mixing ratio of water vapor of the inlet and outlet air, respectively, M_{H2O} [kgmol^{-1}] denotes the molar mass of water, k_V [s^{-1}] denotes the volumetric mass transfer coefficient, V_l [m^3] denotes the two-phase mixing volume in the rectangular bubble column, and Y_{H2O} denotes the water vapour mass fraction of the outlet air:

$$\Delta W_m = \frac{W_1 - W_2}{\ln\left(\frac{W_1 - W_s}{W_2 - W_s}\right)} \tag{6}$$

$$\Delta C_m = \frac{\Delta W_m \rho_g}{M_{H_2O}} \tag{7}$$

where ΔW_m [kgkg^{-1}] is the mass transfer driving force in terms of water vapor difference, W_s [kgkg^{-1}] – the saturation water vapour mixing ratio, which represents the maximum amount of water vapour that dry air can hold at a certain temperature, ΔC_m [molm^{-3}] – the mass transfer driving force in terms of concentration, ρ_g [kgm^{-3}]– the density of dry air at the gas phase inlet.

To systematically investigate the mechanism by which the phase mass transfer coefficient, β, affects the evaporation condensation process, this paper selected five β values of different orders of magnitude (10^{-1}, 10^{-2}, 10^{-3}, 10^{-4}, 10^{-5}) and conducted numerical simulation studies. By comparing the simulation results under different β values, the sensitivity effect on the evaporation condensation process was quantitatively analyzed.

Mechanism of phase change mass transfer coefficient in evaporative processes

Influence of phase change mass transfer coefficient on gas-liquid flow and mass transfer

Numerical simulation results show that the formation and detachment of bubbles during the single-hole bubbling process exhibit distinct periodic characteristics. As shown in fig. 5, by analyzing the volume fraction of water iso-surfaces ($\alpha_l = 0.5$), the periodic evolution of bubbles can be divided into two main stages [29, 30]:

– *Nucleation and expansion stage*: Gas is continuously injected into the liquid phase through the pore opening, first forming a gas nucleus that gradually expands. During this stage, the initial morphology of the bubble is determined by the combined effects of interfacial tension and buoyancy.
– *Detachment and ascent stage*: As the bubble volume increases, buoyancy gradually becomes dominant, causing the neck to contract and narrow, ultimately leading to the bubble ascending and detaching from the pore opening, triggering the start of the next bubbling cycle.

The gas-liquid two-phase flow characteristics exhibit consistent behavior across varying phase change mass transfer coefficients, β. While β predominantly affects the quantitative

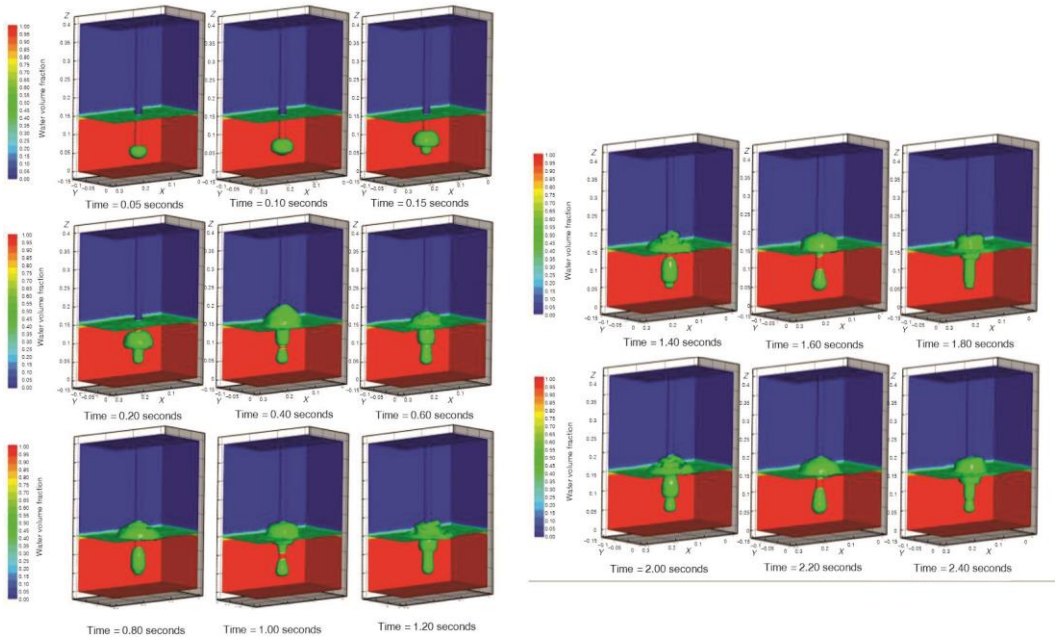

Figure 5. Dynamic evolution process of the gas-liquid interface (α_l = 0.5 iso-surface)

features of the evaporation process at bubble interfaces, its influence on the overall flow structure remains limited. This is attributed to the negligible impact of water vapour content on bubble volume and density. Taking the simulation results at the 0.2 seconds time point under different β values as an example, as shown in fig. 6, the saturation vapour pressure varies synchronously with temperature, achieving dynamic regulation. Furthermore, the following typical mass transfer characteristics can be observed:

– Evaporation occurs in the gas-liquid interface region.
– Water vapour molecules are transported from the liquid phase surface to the gas phase space through convective diffusion.

Based on the heat and mass transfer process involving direct contact between gas and liquid phases, this study focuses on elucidating the dynamic characteristics of evaporation mass transfer at the phase interface. Liquid water undergoes phase change evaporation at the phase interface driven by vapour pressure differences, and the resulting water vapour molecules migrate into the gas phase bulk via diffusion. Taking $\beta = 10^{-5}$ as an example, as shown in fig. 7, as the mass transfer process continues, the system exhibits distinct dynamic evolutionary characteristics: In the initial stage, the mass fraction of water vapour at the outlet region changes significantly over time, then gradually stabilizes, and finally fluctuates slightly around a constant value. This transition from a non-equilibrium state to a quasi-steady state confirms that the system ultimately reaches a dynamic equilibrium state. Figures 8 and 9 show the interfacial volumetric evaporation rate and water vapour concentration distribution under dynamic equilibrium conditions for phase change mass transfer coefficients of $\beta = 10^{-4}$ and $\beta = 10^{-5}$, respectively.

Based on the Lee model source term framework, the improved phase change model retains a single-parameter adjustment structure. By employing a UDF to compute saturation vapour pressure in real time, the mass transfer driving force is replaced from temperature difference

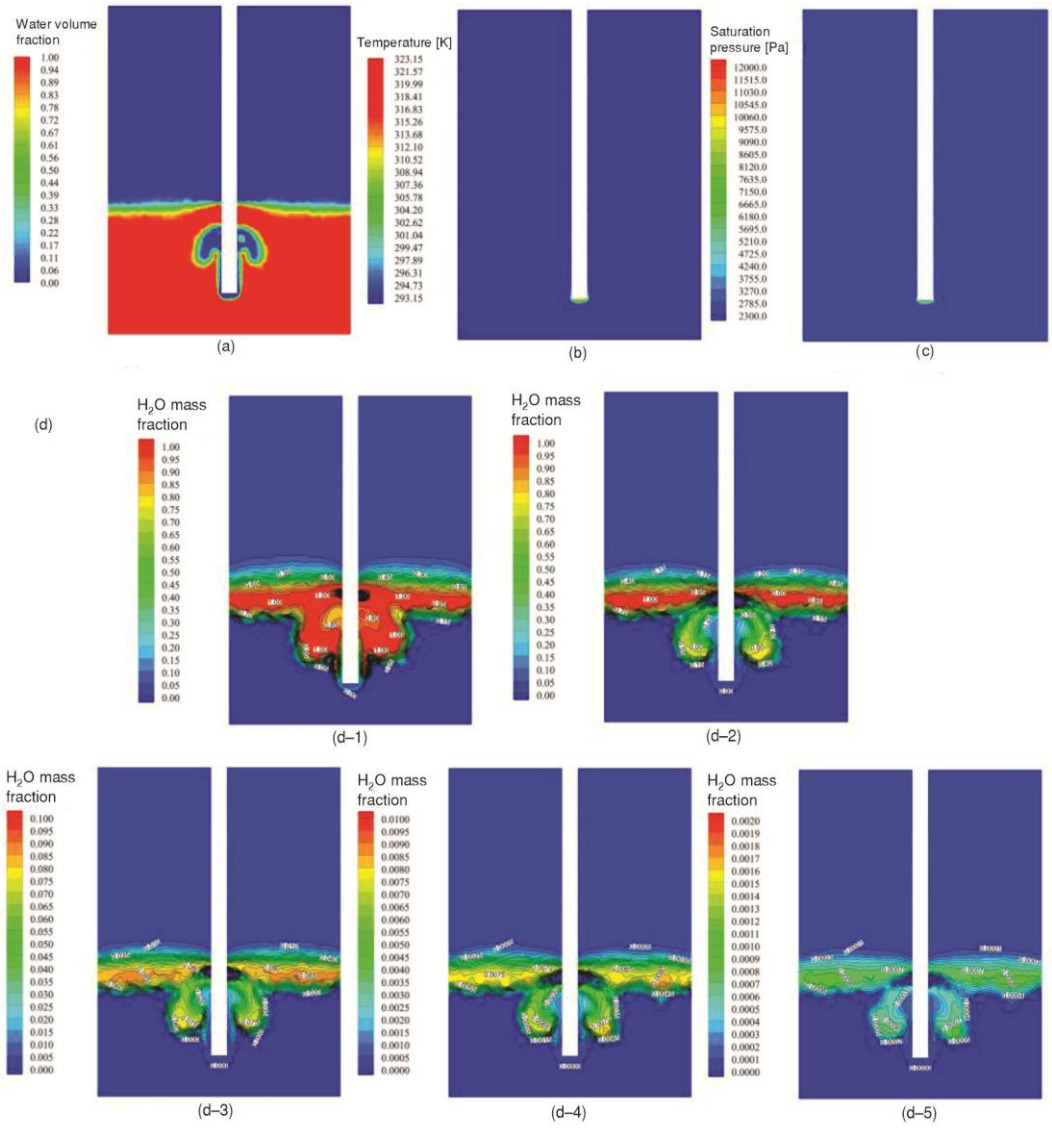

Figure 6. Simulation results for different β values (Time = 0.2 seconds, *xz*-symmetry plane); (a) water volume fraction, (b) temperature, (c) saturation pressure, (d) mass fraction of water vapour (H_2O): (d-1) $\beta = 10^{-1}$, (d-2) $\beta = 10^{-2}$, (d-3) $\beta = 10^{-3}$, (d-4) $\beta = 10^{-4}$, (d-5) $\beta = 10^{-5}$

to vapour pressure difference. This enables evaporation to be driven by humidity difference at unsaturated temperatures. Compared to the original Lee model, which solely employs temperature difference as a criterion, forcing phase transition to cease below saturation temperatures with phase-change mass transfer flux remaining permanently zero, the improved model introduces a dual-criterion mechanism of *temperature-humidity difference*. This enables the maintenance of non-zero mass transfer flux even at atmospheric saturation temperatures (<100 °C), directly validating the effectiveness of the model enhancement. The phase-change mass transfer coefficient requires further experimental refinement and determination.

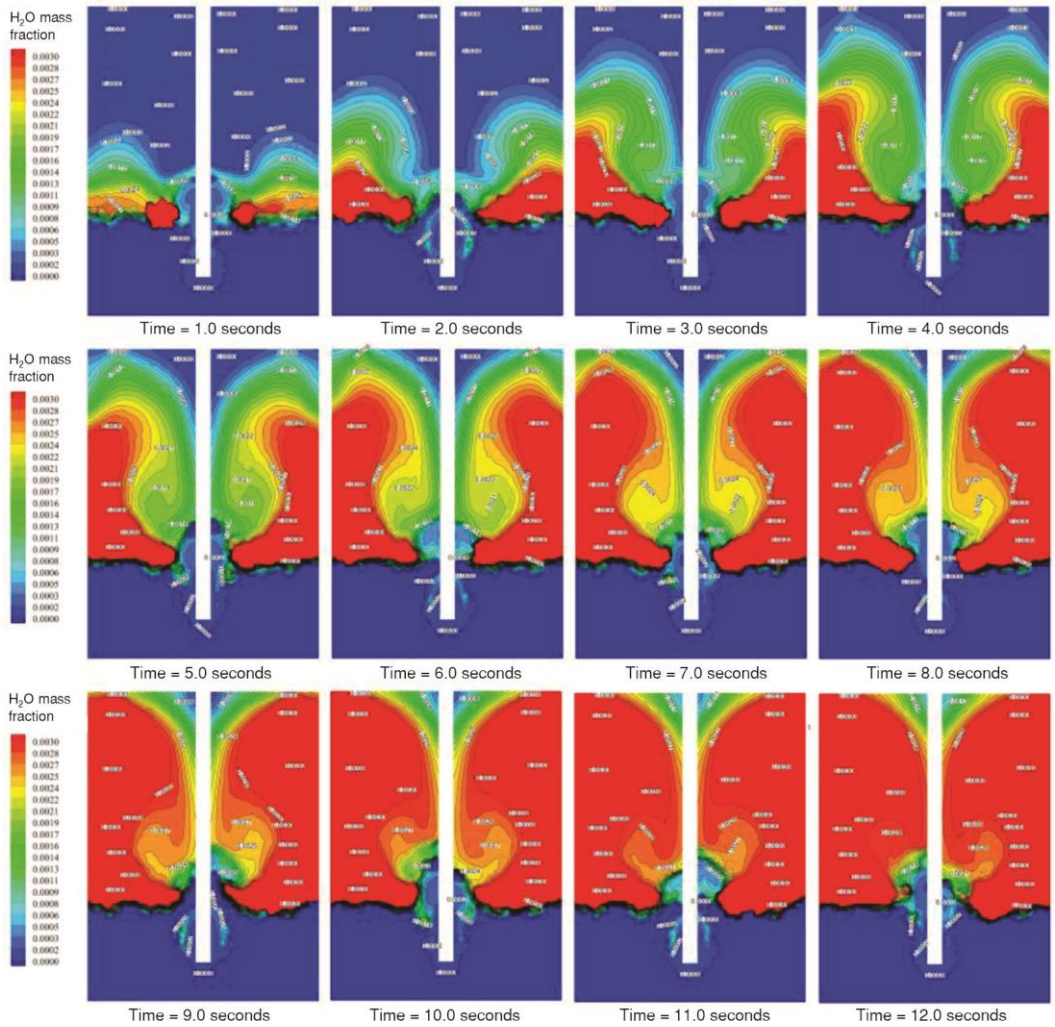

Figure 7. Dynamic evolution of water vapour diffusion during evaporation ($\beta = 10^{-5}$)

Influence of phase change mass transfer coefficient on interfacial mass transfer efficiency and parameter optimisation

Through systematic parameter sensitivity analysis, it was demonstrated that the phase change mass transfer coefficient, β, in the mass transfer model critically governs the transition of mechanism between the gas and liquid phases. Analysis of the mass source term under constant water vapour pressure difference indicates that a lower β value corresponds to reduced mass transfer. A detailed analysis of the influence of the β on the mass transfer process reveals three distinct control stages, as illustrated in fig. 10:

– In the high β value range ($10^{-2} \leq \beta \leq 10^{-1}$), the mass transfer is dominated by the vapour pressure difference. During the quasi-steady-state process, the vapour mass fraction at the air outlet exhibits a slight decrease from 0.49 ±0.01 to 0.46 ±0.01, representing a 6.1% reduction.

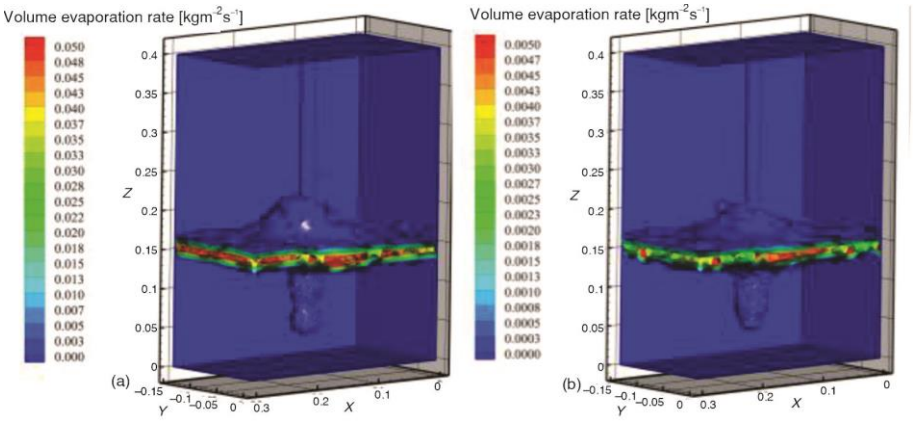

Figure 8. Volume mass transfer rate at the phase interface during quasi-steady state process; (a) $\beta = 10^{-4}$, time = 10.4 seconds and (b) $\beta = 10^{-5}$, time = 13.2 seconds

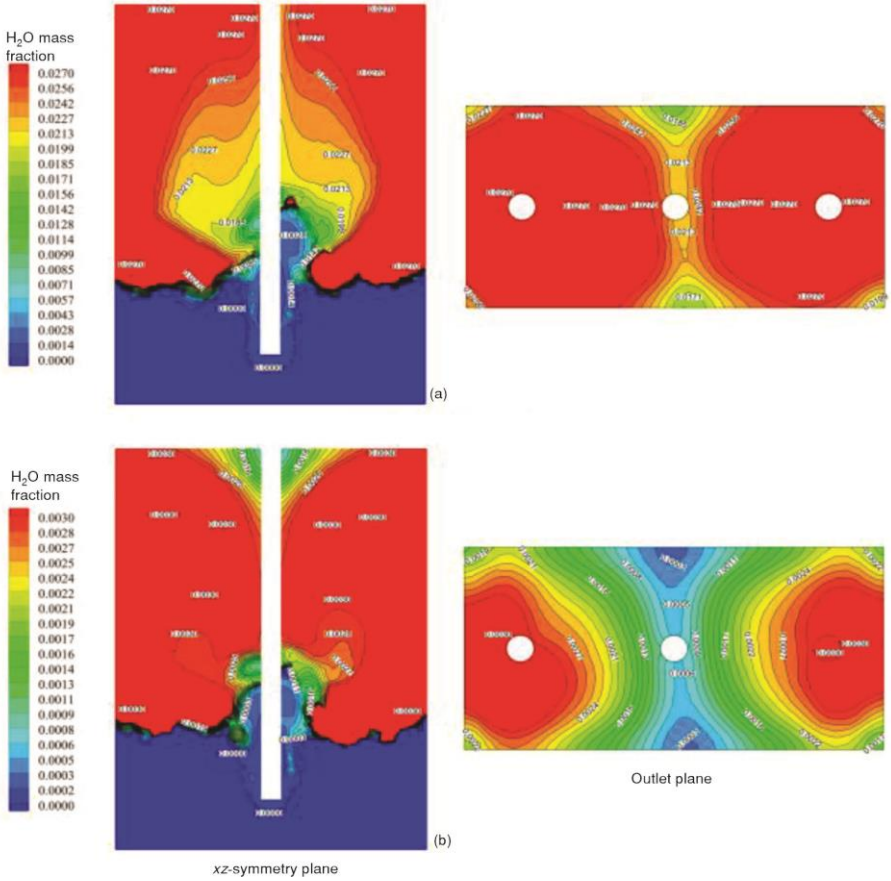

Figure 9. Mass fraction of water vapour in the air during quasi-steady-state processes; (a) $\beta = 10^{-4}$, time = 13.2 seconds and (b) $\beta = 10^{-5}$, time = 13.2 seconds

– When $\beta = 10^{-3}$, the system exhibits a distinct shift in mass transfer mechanisms. At this critical value, β emerges as the dominant factor governing the mass transfer process, with

the outlet water vapour mass fraction exhibiting a sharp decline from 0.46 ±0.01 at $\beta = 10^{-2}$ to 0.19 ±0.01 (a decrease of approximately 60%). Notably, this measured value remains nearly one order of magnitude higher than the theoretical prediction range (0.003-0.0262).

– In the low β value range ($10^{-4} \leq \beta \leq 10^{-5}$), as the system approaches equilibrium, the mass fraction of water vapour in the outlet air stabilizes within the range of 0.003-0.036. This measured result is in good agreement with the back-calculated predicted value (0.003-0.0262) based on the volumetric mass transfer coefficient, with a correlation of over 92.3%.

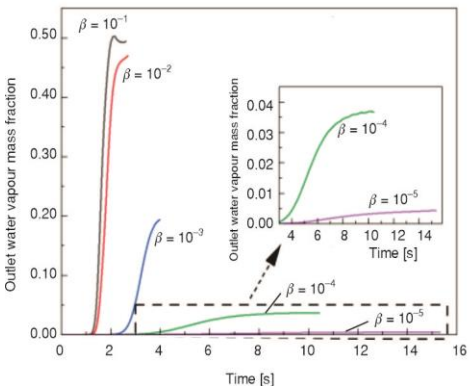

Figure 10. Temporal evolution of outlet water vapour mass fraction

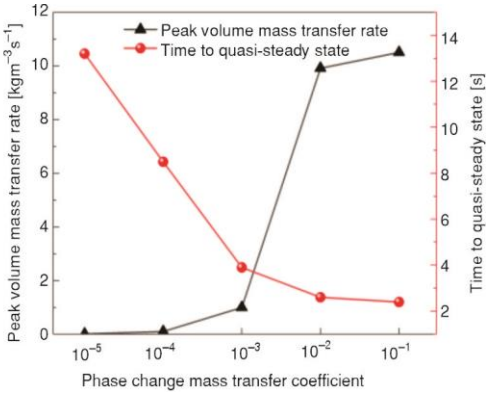

Figure 11. Effect of β on the peak volume mass transfer rate and time to quasi-steady state

Furthermore, as a key mass transfer parameter, β exerts significant influence on both the peak volumetric mass transfer rate and the system's equilibration time characteristics, fig. 11. For $\beta < 10^{-3}$, the peak volumetric mass transfer rate exhibits exponential growth with increasing β values, showing nearly an order-of-magnitude enhancement. In contrast, when $\beta > 10^{-3}$, the mass transfer rate variation becomes relatively stable, with merely a 6% increment. The behavior demonstrates the pronounced dependence of the mass transfer process on β values over time. Notably, when β crosses the critical threshold of 10^{-3}, the equilibration time of the system exhibits a step-change characteristic. Specifically, the gas-liquid mass transfer process takes over twice as long to reach equilibrium in the high β regime as in the low β regime.

Conclusions and future perspectives

This study established an improved low-temperature evaporation model based on the theoretical framework of Lee's model by introducing dynamic equilibrium constraints between the partial pressure of water vapour and the saturated pressure at the phase interface. Using parameter sensitivity analysis, the influence of the phase change mass transfer coefficient, β, on the evaporation mass transfer process was determined:

- The mass transfer rate is positively correlated with the β value. An increase in the β value leads to an increase in the mass of evaporation, as well as a corresponding increase in the mass fraction of water vapour in the outlet air.
- In the high β value range (10^{-1} to 10^{-2}), the mass transfer process is primarily driven by the vapour pressure difference, with the β value has a slight impact.
- A significant change in the characteristics of mass transfer was observed at $\beta = 10^{-3}$. In the low-temperature evaporation model, the dominant mechanism of mass transfer transitioned from vapour pressure control to β-value control.

- In the low β value range (10^{-4} to 10^{-5}), β becomes the mass transfer limiting factor and changes in β directly affect a significant decrease in phase change mass transfer.

An improved low temperature evaporation model was used to conduct numerical simulations of the dry air-water single-pore bubbling evaporation process. This yielded an applicable range for the phase change mass transfer coefficient, β, of 10^{-4} to 10^{-5} under this system. It is worth noting that numerical simulations of condensation processes involving strong coupling effects among multiple physical fields (flow, temperature, and composition) face greater convergence challenges than evaporation processes.

Nomenclature

C_m – concentration, [molm^{-3}]
H – latent heat, [Jkg^{-1}]
M_{H2O} – molar mass of H_2O, [kgmol^{-1}]
$\dot{m}_G$ – mass-flow rate, [kgs^{-1}]
N_A – mass transfer rate, [mols^{-1}]
P – pressure, [Pa]
S – mass source term, [kgm^{-3}s^{-1}]
T – temperature, [K]
V – volume, [m^3]
W – water vapour mixing ratio, [kgkg^{-1}]
Y_{H2O} – water vapour mass fraction

Greek symbols

α – volume fraction
β – phase change mass transfer coefficient, [s^{-1}]
ρ – density, [kgm^{-3}]

Subscripts

c - condensation
e – evaporation
l – liquid
sat – saturation
v – vapor

References

[1] Polikarpov, A. Ph., *et al*., Kinetic Simulation of the Non-Equilibrium Effects at the Liquid-Vapor Interface, *International Journal of Heat and Mass Transfer*, *136* (2019), June, pp. 449-456
[2] Matsunaga, N., Nagashima, A., Saturation Vapor Pressure and Critical Constants of H_2O, D_2O, T_2O, and their Isotopic Mixtures, *Int. J. Thermophys*, *8* (1987), 6, pp. 681-694
[3] Hirt, C. W., Nichols, B. D., Volume of Fluid (VOF) Method for the Dynamics of Free Boundaries, *Journal of Computational Physics*, *39* (1981), 1, pp. 201-225
[4] Xu, L., *et al*., Numerical Simulation of Motion Behavior of Single Bubble Rising in Still Water, *Journal of Shenyang Agricultural University*, *43* (2012), 3, pp. 357-361
[5] Tomiyama, A., *et al*., Numerical Analysis of Bubble Motion with the VOF Method, *Nuclear Engineering and Design*, *141* (1993), 1-2, pp. 69-82
[6] Gadala, M. S., *et al*., A 3-Dimenional CFD Study of Boiling in Jet Impingement, *Heat Mass Transfer*, *60* (2024), 7, pp. 1145-1158
[7] Jeon, S.-S., *et al*., CFD Simulation of Condensing Vapor Bubble Using VOF Model, *World Academy of Science, Engineering & Technology*, *60* (2009), Dec., pp. 209-215
[8] Van Sint Annaland, M., *et al*., Numerical Simulation of Gas Bubbles Behaviour Using a Three-Dimensional Volume of Fluid Method, *Chemical Engineering Science*, *60* (2005), 11, pp. 2999-3011
[9] Qiu, G., *et al*., Analysis on the Value of Coefficient of Mass Transfer with Phase Change in Lee's Equation (in Chinese), *Journal of Harbin Institute of Technology*, *46* (2014), 12, pp. 15-19
[10] Ruan, Y., *et al*., Numerical Simulation of Evaporation Heat Transfer Characteristics Within Bubble Plate Heat Exchanger Based on VOF Method, *Chemical Engineering (China)*, *53* (2025), 3, pp. 40-45
[11] Saleem, A., *et al*., Wall Superheat at the Incipient Nucleate Boiling Condition for Natural and Forced Convection: A CFD Approach, *Computers & Chemical Engineering*, *134* (2020), Mar., pp. 106718
[12] Soleimani, A., *et al*., Thermal Analysis of a Microchannel Heat Sink Cooled by Two-Phase Flow Boiling of Al_2O_3 HFE-7100 Nanofluid, *Thermal Science and Engineering Progress*, *20* (2020), 100693
[13] Yang, Z., *et al*., Numerical and Experimental Investigation of Two Phase Flow During Boiling in a Coiled Tube, *International Journal of Heat and Mass Transfer*, *51* (2008), 5-6, pp. 1003-1016
[14] Zhang, Y., *et al*., Development and Modified Implementation of Lee Model for Condensation Simulation, *Applied Thermal Engineering*, *231* (2023), 120872

[15] Shen, Q., *et al*., Development of Heat and Mass Transfer Model for Condensation, *International Communications in Heat and Mass Transfer*, *84* (2017), May, pp. 35-40
[16] Sun, Y., *et al*., Development of an Improved Mass Transfer Model for Condensation with Dynamic Feedback Regulation, *International Journal of Heat and Mass Transfer*, *236* (2025), 126266
[17] Alizadehdakhel, A., *et al*., CFD Modeling of Flow and Heat Transfer in A Thermosyphon, *International Communications in Heat and Mass Transfer*, *37* (2010), 3, pp. 312-318
[18] Cheng, Z., *et al*., Experimental and Numerical Study of Flow Boiling in a Vertical Upward Narrow Rectangular Channel Under Low Heat Flux, *Applied Thermal Engineering*, *256* (2024), 124149
[19] Luo, Y., *et al*., A Comparative Numerical Study on Two-Phase Boiling Fluid Flow and Heat Transfer in the Microchannel Heat Sink with Different Manifold Arrangements, *Int. J. Heat Mass Transf.*, *156* (2020), 119864
[20] Chen, S., *et al*., Simulation of Condensation Flow in a Rectangular Microchannel, *Chemical Engineering and Processing: Process Intensification*, *76* (2014), Feb., pp. 60-69
[21] Wang, X., *et al*., Development of Pressure-Based Phase Change Model for CFD Modelling of Heat Pipes, *International Journal of Heat and Mass Transfer*, *145* (2019), 118763
[22] Liu, H., *et al*., Advancements in Energy-Efficient Building Technologies: An Enhanced Lee Model for Precision Simulation and Optimization of Heat Pipe Applications, *J. of Building Eng.*, *88* (2024), 109026
[23] Zhang, C., *et al*., Experimental Study of a Novel Double-Effect Evaporation Concentration System for High Temperature Heat Pump, *Desalination*, *491* (2020), 114495
[24] Lee, W. H., A Pressure Iteration Scheme for Two-Phase Flow Modeling, *Multiphase Transport Fundamentals, Reactor Safety, Applications*, *1* (1980), pp. 407-431
[25] Wagner, W., Pruß, A., The IAPWS Formulation 1995 for the Thermodynamic Properties of Ordinary Water Substance for General and Scientific Use, *J. Phys. Chem. Ref. Data*, *31* (2002), 2, pp. 387-535
[26] Hui, L., Hong, X., Comparison of Antoine Equation Constants for Water Vapour Pressure Saturation, *Inner Mongolia Petroleum & Chemical Industry*, *35* (2009), 13, pp. 32-34
[27] Brackbill, J. U., *et al*., A Continuum Method for Modeling Surface Tension, *Journal of Computational Physics*, *100* (1992), 2, pp. 335-354
[28] Zhang, X., Research on Simultaneous Heat and Mass Transfer Process in Bubbling Tower, Ph. D. thesis, Zhejiang University, Zhejiang, China, 2022
[29] Chen, W., *et al*., Numerical Simulation of Underwater Air Bubble Formation Under Rolling Conditions, *Annals of Nuclear Energy*, *143* (2020), 107451
[30] Zhang, Y., *et al*., Three-Dimensional Volume of Fluid Simulations on Bubble Formation and Dynamics in Bubble Columns, *Chemical Engineering Science*, *73* (2012), May, pp. 55-78

Paper submitted: October 3, 2025
Paper revised: November 28, 2025
Paper accepted: December 2, 2025

2026 Published by the Vinča Institute of Nuclear Sciences, Belgrade, Serbia.
This is an open access article distributed under the CC BY 4.0 terms and conditions.